Bulgarian Journal of Physics vol. **XX** (20XX) 1–15

# A New Approach for Studying the Isoscalar Giant Monopole Resonance

**M.K. Gaidarov**[1,2*], **M.V. Ivanov**[1,2] **Y.I. Katsarov**[1] **A.N. Antonov**[1]

[1]Institute for Nuclear Research and Nuclear Energy,
Bulgarian Academy of Sciences, Sofia 1784, Bulgaria

[2]Department of Physics, Faculty of Mathematics and Natural Sciences,
Neofit Rilski South-West University, Blagoevgrad, Bulgaria

[*]Corresponding author Email: gaidarov@inrne.bas.bg

Received *5 March 2025*

**Abstract.** A systematic study of the isoscalar giant monopole resonance (ISGMR) in spherical and deformed nuclei from various isotopic chains is performed within the microscopic self-consistent Skyrme HF+BCS method and coherent density fluctuation model. The calculations for the incompressibility in finite nuclei are based on the Brueckner energy density functional for nuclear matter. The good agreement achieved between the calculated centroid energies of the ISGMR and their recent experimental values for various nuclei demonstrate the relevance of the proposed theoretical approach. The latter can be applied to analyses of neutron stars properties, such as incompressibility, symmetry energy, slope parameter, and other astrophysical quantities.

KEY WORDS: energy density functional, equation of state, finite nuclei, incompressibility, nuclear monopole excitation, nuclear matter, symmetry energy.

## 1 Introduction

The study of giant resonances, particularly the isoscalar giant monopole resonance (ISGMR) [1,2], is indeed fascinating. These resonances provide valuable insights into the collective behavior of nuclei and are crucial for understanding the nuclear equation of state (EOS). The energy of the ISGMR is closely linked to nuclear incompressibility, which in turn is related to the incompressibility of infinite nuclear matter-a key component of the EOS [2–7].

The EOS is essential for describing various astrophysical phenomena, such as radii and masses of neutron stars, collapse of massive stars in supernova explosions, and for the modelling of heavy ion collisions. However, there is a significant uncertainty (around 20%) in the current value of nuclear matter incompressibility, mainly due to the poorly defined isospin asymmetry term in the EOS.

 

To address this, recent experimental measurements of isoscalar monopole modes have been extended to isotopic chains, moving from stable nuclei to exotic ones with greater proton-neutron asymmetry. This helps to refine the isospin asymmetry term and to improve our understanding of the EOS.

Isoscalar resonances are excited via low-momentum transfer reactions in inverse kinematics, for which unique detection devices are necessary. Currently, active targets have yielded promising results. Measurements on Ni isotopes far from stability, specifically $^{56}$Ni and $^{68}$Ni [8, 9], have been performed. Notably, the $^{68}$Ni [10, 11] experiment marked the first measurement of isoscalar monopole response in a short-lived neutron-rich nucleus through inelastic alpha-particle scattering. The ISGMR peak appeared fragmented, suggesting the potential presence of a soft monopole resonance. Discussions on deriving the incompressibility of nuclear matter, $\Delta K^{\rm NM}$, from the ISGMR have been ongoing since the 1980s [12, 13]. The measurement of the ISGMR's centroid energy is a highly sensitive method for determining $\Delta K^{\rm NM}$'s value [14–20]. Various theoretical models that group values of $\Delta K^{\rm NM}$ predict different ISGMR energies [21–27], which, when compared with experimental data, can constrain the incompressibility of nuclear matter.

In this study, the nuclear incompressibility and the centroid energy of ISGMR are examined by applying the Brueckner energy-density functional for nuclear matter [28, 29] and the coherent density fluctuation model (CDFM) [30, 31]. The CDFM, an extension of the Fermi gas model derived from the delta-function limit of the generator coordinate method, incorporates long-range collective correlations [32,33]. Over the years, the CDFM has been effectively used for calculating characteristics of nuclear structure and reactions. Noteworthy are the calculated energies, density distributions, and rms radii of the ground states in $^{4}$He, $^{16}$O, and $^{40}$Ca nuclei [34]. Specifically, the CDFM has been used to calculate the energies of breathing monopole states in $^{16}$O, $^{40}$Ca, $^{90}$Zr, $^{116}$Sn, and $^{208}$Pb [35]. Regarding reaction properties, the CDFM has been employed to calculate the scaling function in nuclei using the relativistic Fermi gas scaling function, applicable to lepton scattering processes [36]. It has also provided insights into the role of nucleon momentum and density distributions in explaining superscaling in lepton-nucleus scattering [37, 38], as well as in analyzing cross sections for various reactions: inclusive electron scattering in the quasielastic region and neutrino (antineutrino) scattering for both charge-changing and neutral-current processes [39–42]. Additionally, the CDFM has been used to investigate the scaling function's relationship with the spectral function and nucleon momentum distribution [43]. The CDFM has proven its efficiency as a "bridge" for a transition from the properties of nuclear matter to those of finite nuclei, studying nuclear symmetry energy (NSE), neutron pressure, and asymmetric compressibility in finite nuclei [44–46].

In this study, we conduct calculations and present results for ISGMR excitation energies of Ni, Sn, and Pb isotopes. Our primary objective is to validate the CDFM for the analysis of collective vibrational modes, employing the self-consistent Hartree-Fock (HF)+BCS method with Skyrme interactions. The CDFM establishes a link between nuclear matter and finite nuclei for investigation of their characteristics across light, medium, and heavy nuclei. For instance, we use the energy density functional (EDF) of Brueckner *et al.* [28, 29] for nuclear matter. It is evident that future research should implement more realistic functionals, which are expected to yield ISGMR excitation energy values that align more closely with experimental data. We study the evolution of the centroid energy values within the Sn isotopic chain ($A$=112-124), focusing on its isotopic sensitivity. The selection of these chains of spherical nuclei is partially based on recent extensive ISGMR measurements, hence our emphasis on comparing our findings with existing experimental data for Ni [47], Sn [48], and Pb [49, 50] isotopes. Furthermore, we compare the centroid energy values of ISGMR for Ca, Fe, Zn, Zr, Mo, and Cd isotopes derived from HF+BCS calculations using the SLy4 and SkM Skyrme forces with the available experimental data.

In Section 2, we define the excitation energy of ISGMR and the EOS parameters of nuclear matter, which characterize its density dependence near normal nuclear matter density. We also provide a concise description of the CDFM formalism, which facilitates the calculation of finite nuclei quantities. The numerical results are presented and discussed in Section 3, while the main conclusions of the study are summarized in Section 4.

## 2 Theoretical Scheme

### 2.1 Excitation energy of the ISGMR

The centroid energy of the ISGMR, $E_{\text{ISGMR}}$, is typically associated with the incompressibility $\Delta K(N,Z)$ for a nucleus with $Z$ protons and $N$ neutrons ($A = Z+N$ is the mass number). Among the different definitions of $E_{\text{ISGMR}}$ we refer to the one from, for example Ref. [21]):

$$E_{\text{ISGMR}} = \frac{\hbar}{r_0 A^{1/3}}\sqrt{\frac{\Delta K(N,Z)}{m}}, \tag{1}$$

where $r_0$ is deduced from the equilibrium density and $m$ denotes the nucleon mass. Additionally, the excitation energy of the ISGMR is described in the scaling model as [15, 16, 51]:

$$E_{\text{ISGMR}} = \hbar\sqrt{\frac{\Delta K(N,Z)}{m\langle r^2\rangle}}, \tag{2}$$

where $\langle r^2\rangle$ denotes the mean square mass radius of the nucleus in the ground state. The value of $E_{\text{ISGMR}}$ varies according to the chosen model, correlating with different moment ratios of the ISGMR strength distribution. The primary goal of related experiments is to determine this value, thereby restricting the incompressibility of infinite nuclear matter and, consequently, the EOS [13]. It is important to note that the definition (2) is valid only if the strength distribution for a specific multipolarity of the resonance is confined to a singular collective peak [18].

### 2.2 The EOS parameters for nuclear matter

The symmetry energy, $S(\rho)$, is characterized by the energy per particle in nuclear matter (NM) $E(\rho,\delta)$:

$$S(\rho) = \frac{1}{2}\left.\frac{\partial^2 E(\rho,\delta)}{\partial\delta^2}\right|_{\delta=0}, \tag{3}$$

where

$$E(\rho,\delta) = E(\rho,0) + S(\rho)\delta^2 + O(\delta^4) + \cdots \tag{4}$$

and

$$\delta = (\rho_n - \rho_p)/\rho \tag{5}$$

is a function of the isospin asymmetry. The baryon density is given by:

$$\rho = \rho_n + \rho_p, \tag{6}$$

where $\rho_n$ and $\rho_p$ represent the densities of neutrons and protons [52–54]).

The incompressibility or the curvature of the symmetry energy is:

$$\Delta K^{\mathrm{NM}} = 9\rho_0^2 \left.\frac{\partial^2 S}{\partial\rho^2}\right|_{\rho=\rho_0}, \tag{7}$$

where $\rho_0$ is the density at equilibrium.

### 2.3 The EOS parameters for finite nuclei within the coherent density fluctuation model

The CDFM was proposed and elaborated in Refs. [30–32] (see, e.g., [44,45,52,55]). Within this model, the one-body density matrix (OBDM) of the nucleus is:

$$\rho(\mathbf{r},\mathbf{r}') = \int_0^\infty dx|F(x)|^2\rho_x(\mathbf{r},\mathbf{r}'). \tag{8}$$

The OBDM $\rho(\mathbf{r},\mathbf{r}')$ of the nucleus is a superposition of OBDM's $\rho_x(\mathbf{r},\mathbf{r}')$ of spherical "pieces" of nuclear matter (called "fluctons") with radius $x$ in which all A nucleons are uniformly distributed:

$$\rho_x(\mathbf{r},\mathbf{r}') = 3\rho_0(x)\frac{j_1(k_F(x)|\mathbf{r}-\mathbf{r}'|)}{(k_F(x)|\mathbf{r}-\mathbf{r}'|)}\Theta\left(x - \frac{|\mathbf{r}+\mathbf{r}'|}{2}\right), \tag{9}$$

where $j_1$ is the first-order spherical Bessel function and

$$k_F(x) = \left(\frac{3\pi^2}{2}\rho_0(x)\right)^{1/3} \equiv \frac{\alpha}{x} \tag{10}$$

is the Fermi momentum. In Eq. (10)

$$\alpha \equiv \left(\frac{9\pi A}{8}\right)^{1/3} \simeq 1.52A^{1/3}. \tag{11}$$

The nucleon density distribution is given by the diagonal elements of the OBDM (8):

$$\rho(\mathbf{r}) = \int_0^\infty dx|F(x)|^2\rho_0(x)\Theta(x-|\mathbf{r}|) \tag{12}$$

with

$$\rho_0(x) = \frac{3A}{4\pi x^3}. \tag{13}$$

It follows from Eq. (12) that the weight function $|F(x)|^2$ of CDFM can be obtained in the case of monotonically decreasing local densities (*i.e.*, for $\dfrac{d\rho(r)}{dr} \leq 0$) by

$$|F(x)|^2 = -\frac{1}{\rho_0(x)}\left.\frac{d\rho(r)}{dr}\right|_{r=x} \tag{14}$$

being normalized as

$$\int_0^\infty dx|F(x)|^2 = 1. \tag{15}$$

In the case of the Brueckner method for nuclear matter energy [21, 28, 29] the symmetry energy $S^{\mathrm{NM}}(x)$ and the asymmetric incompressibility $K^{\mathrm{NM}}(x)$ have the form (see Refs. [45, 55]):

$$S^{\mathrm{NM}}(x) = 41.7\rho_0^{2/3}(x) + b_4\rho_0(x) + b_5\rho_0^{4/3}(x) + b_6\rho_0^{5/3}(x), \tag{16}$$

$$\Delta K^{\mathrm{NM}}(x) = -83.4\rho_0^{2/3}(x) + 4b_5\rho_0^{4/3}(x) + 10b_6\rho_0^{5/3}(x). \tag{17}$$

According to the CDFM scheme, the symmetry energy and the curvature for finite nuclei can be expressed in the following form:

$$s = \int_0^\infty dx|F(x)|^2 S^{\mathrm{NM}}(x), \tag{18}$$

$$\Delta K = \int_0^\infty dx|F(x)|^2 \Delta K^{\mathrm{NM}}(x). \tag{19}$$

In our calculations, we employ the self-consistent Hartree-Fock method with density-dependent Skyrme interactions [56] and pairing correlations. We utilize the Skyrme SLy4, Sk3, SGII parametrizations [57–59] and the SkM parameter set [60], which provide an accurate description of bulk nuclear properties (see also [44–46, 55, 61, 62]). All necessary expressions for the single-particle functions and densities in the HF+BCS method can be found, e.g., in Ref. [45].

It is known that the value of the nuclear matter incompressibility $\Delta K^{\mathrm{NM}}$ plays a key role in determining the location of the ISGMR centroid energy [48]. The different Skyrme parameter sets used in the present calculations are chosen since they are characterized by different values of the nuclear incompressibility, $\Delta K^{\mathrm{NM}} = 230$, 217, 215, and 355 MeV for SLy4, SkM, SGII, and Sk3, respectively [63].

## 3 Results

First, in Figure 1 we overlay, as examples, the density distributions of $^{56}$Ni and $^{208}$Pb and the corresponding CDFM weight function $|F(x)|^2$ as a function of $x$. As mentioned before, the densities are obtained in a self-consistent Hartree–Fock+BCS calculations with SLy4 interaction. The function $|F(x)|^2$ which is used in Eq. (19) to obtain the incompressibility modulus, which is necessary to calculate the $E_{\mathrm{ISGMR}}$, has the form of a bell with a maximum around $x = R_{1/2}$ at which the value of the density $\rho(x = R_{1/2})$ is around half of the value of the central density equal to $\rho_c$ [$\rho(R_{1/2})/\rho_c = 0.5$]. It was shown in Refs. [52, 55] that in this region around $\rho = \rho_c/2$ the values of $\Delta K^{\mathrm{NM}}(\rho)$ take a significant part in the calculations. This fact is of particular importance and is related to the behavior of $S^{\mathrm{NM}}(x)$ [Eq. (16)] in the case of the Brueckner EDF showing its isospin instability (see Fig. 1 of Ref. [52]), in contrast with other more realistic energy-density functionals. Therefore, to fully specify the role of both quantities $\Delta K^{\mathrm{NM}}[\rho_0(x)]$ and $|F(x)|^2$ in the expression (19) for the finite nuclei incompressibility $\Delta K$ and to locate the relevant region of densities in finite

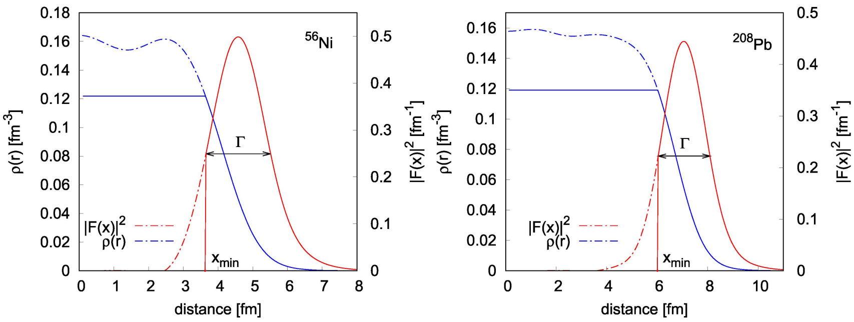


Figure 1. The densities $\rho(r)$ (in fm$^{-3}$) of $^{56}$Ni and $^{208}$Pb calculated in the Skyrme HF + BCS method with SLy4 force (normalized to $A = 56$ and $A = 208$, respectively) and the weight function $|F(x)|^2$ (in fm$^{-1}$) normalized to unity [Eq. (15)].

nucleus calculations, we apply the same physical criterion related to the weight function $|F(x)|^2$, as in [52]. This is the width $\Gamma$ of the weight function $|F(x)|^2$ at its half maximum (which is illustrated in Figure 1 on the example of $^{56}$Ni and $^{208}$Pb nuclei together with the corresponding distance in the density distribution $\rho(r)$), which is a good and acceptable choice. More specifically, we define the lower limit of integration as the lower value of the radius $x$, $x_{\rm min}$, corresponding to the left point of the half-width $\Gamma$ (for more details see the discussion in Refs. [52, 55]). One can see also in Figure 1 the part of the density distribution $\rho(r)$ (at $r \geq x_{\rm min}$) that is involved in the calculations.

The centroid positions of the monopole mode obtained in this work are compared with available experimental data in Tables 1–3. The calculated values of $E_{\rm ISGMR}$ with SLy4 and SkM forces for Ni and Pb isotopes are given in Tables 1 and 3, respectively. The values of the centroid energies for Sn isotopes obtained from calculations with three Skyrme interactions (SLy4, SGII, Sk3) are listed in Table 2. It can be seen from Table 1 that a very good agreement with the experimental data for $^{56,58,60}$Ni is obtained, while the results with both Skyrme interactions underestimate the experimental energy of the soft monopole vibrations of $^{68}$Ni. The excitation energy of this ISGMR in $^{68}$Ni is located unexpectedly at higher energy (21.1 MeV) for the Ni isotopic chain, having at the same time

Table 1. The values of the centroid energies $E_{\rm ISGMR}$ (in MeV) of Ni isotopes obtained from HF+CDFM calculations in this work using SLy4 and SkM Skyrme forces compared with the experimental data found in the literature.

| **Nucleus** | **SLy4** | **SkM** | **Exp.** |
|---|---|---|---|
| $^{56}$Ni | 19.41 | 19.57 | 19.1 $\pm$ 0.5 [9] |
| | | | 19.3 $\pm$ 0.5 [8] |
| $^{58}$Ni | 18.95 | 19.18 | 18.43 $\pm$ 0.15 [47] |
| $^{60}$Ni | 18.62 | 18.79 | 18.10(29) [47] |
| $^{68}$Ni | 17.46 | 17.70 | 21.1 $\pm$ 1.9 [10, 11] |

Table 2. The values of the centroid energies $E_{\rm ISGMR}$ (in MeV) of Sn isotopes ($A$=112-124) obtained from HF+CDFM calculations in this work using SLy4, SGII, and Sk3 Skyrme forces. The experimental data are taken from Table III of Ref. [48].

| **Nucleus** | **SLy4** | **SGII** | **Sk3** | **Exp.** |
|---|---|---|---|---|
| $^{112}$Sn | 15.04 | 15.30 | 14.89 | 16.2 $\pm$ 0.1 |
| $^{114}$Sn | 15.03 | 15.20 | 14.70 | 16.1 $\pm$ 0.1 |
| $^{116}$Sn | 14.94 | 15.08 | 14.56 | 15.8 $\pm$ 0.1 |
| $^{118}$Sn | 14.82 | 15.13 | 14.48 | 15.8 $\pm$ 0.1 |
| $^{120}$Sn | 14.69 | 15.08 | 14.58 | 15.7 $\pm$ 0.1 |
| $^{122}$Sn | 14.68 | 15.00 | 14.61 | 15.4 $\pm$ 0.1 |
| $^{124}$Sn | 14.68 | 14.96 | 14.51 | 15.3 $\pm$ 0.1 |

Table 3. The values of the centroid energies $E_{\text{ISGMR}}$ (in MeV) of Pb isotopes obtained from HF+CDFM calculations in this work using SLy4 and SkM Skyrme forces compared with the experimental data found in the literature.

| **Nucleus** | **SLy4** | **SkM** | **Exp.** | **Theory** |
|---|---|---|---|---|
| $^{204}$Pb | 12.16 | 12.29 | 13.98 [49] | |
| $^{206}$Pb | 12.12 | 12.23 | 13.94 [49] | |
| $^{208}$Pb | 12.10 | 12.15 | 13.96±0.2 [50] | 14.453 [23] |

large error bars. The reason is due to the large fragmentation of the isoscalar monopole strength in the unstable neutron-rich $^{68}$Ni nucleus, much more than in stable nuclei [10, 11]. The obtained values of $E_{\text{ISGMR}}$ for Sn isotopes ($A$ = 112–124) exhibit small difference regarding the Skyrme parametrization (see Table 2). The theoretical results for the centroid energies for the same Sn isotopes obtained in Ref. [48] by using the SkP (between 14.87 and 15.60 MeV), SkM* (between 15.57 and 16.23 MeV), and SLy5 (between 15.95 and 16.61 MeV) parameter sets are in good agreement with our results. Almost no dependence on the Skyrme forces used in the calculations of the centroid energies is found for Ni and Pb isotopes being slightly larger in the case of SkM interaction than when using the SLy4 one.

The collective nature of giant resonances and nuclear incompressibility suggests a relatively smooth variation in the properties of the ISGMR with mass, indicating that strong variations due to internal nuclear structure are not anticipated. The isotopic evolution of the centroid energies $E_{\text{ISGMR}}$ for Ni, Sn, and Pb isotopes is presented in Figure 2 in the case when $r_0 = 1.2$ fm is used. In general, as expected, a smooth decrease in the excitation energies of the ISGMR with the increase in the mass number $A$ is observed for the three isotopic chains and for all Skyrme forces used in the calculations. Furthermore, going from Ni to Pb isotopic chain the "gap" between our results and the corresponding experimental data becomes larger in a way that the obtained values of $E_{\text{ISGMR}}$ underestimate the experimentally extracted values. Nevertheless, this difference does not exceed 1–2 MeV in the case of Sn and Pb isotopes and practically is minimal for Ni isotopes.

To examine the influence of the half-density radius parameter $r_0$ on the centroid energy [Eq. (1)], we present in Figure 3 the results of $E_{\text{ISGMR}}$ for the same Ni, Sn, and Pb isotopic chains in the case of SLy4 force obtained with two more values of $r_0$. In addition to the results with $r_0 = 1.2$ fm (e.g., in Refs. [64, 65]) given in Figure 2, the values of $E_{\text{ISGMR}}$ calculated with $r_0 = 1.07$ fm (for instance, in Ref. [66]) and $r_0 = 1.123$ fm [67] are shown in Figure 3. It is seen from the figure that with the increase of $r_0$ the agreement with the experimental data becomes better for lighter isotopes. Particularly, the value of $r_0 = 1.123$ fm leads to fair agreement of the ISGMR energies for Sn isotopes, while for Ni isotopes the experimental data are reproduced better with $r_0 = 1.2$

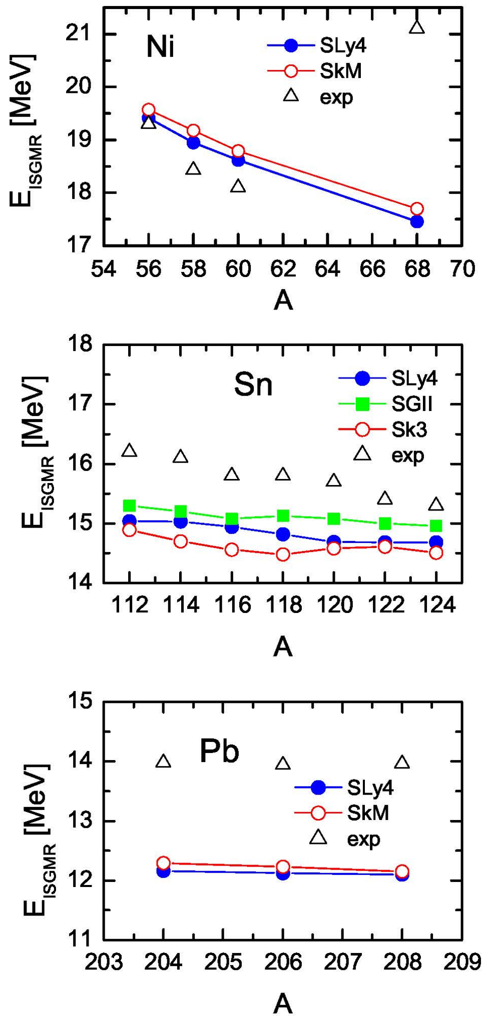


Figure 2. The centroid energies $E_{\text{ISGMR}}$ as a function of the mass number $A$ for Ni, Sn, and Pb isotopes in the cases of SLy4, SGII, Sk3, and SkM forces and $r_0 = 1.2$ fm [Eq. (1)] compared with the experimental data.

fm and for Pb isotopes with $r_0 = 1.07$ fm. Here we would like to note that the specific choice of the $r_0$ parameter values adopted to calculate the values of the centroid energies by using expression (1) is often used in the literature. The values of the measured nuclear radii are deduced from processes with strongly interacting particles or electron (muon) scattering. It is well known that the $A$-dependence of $r_0$ exhibits a smooth decrease with $A$ being 1.07 fm for nuclei with $A > 16$ and increasing to 1.2 fm for heavy nuclei. This results on the

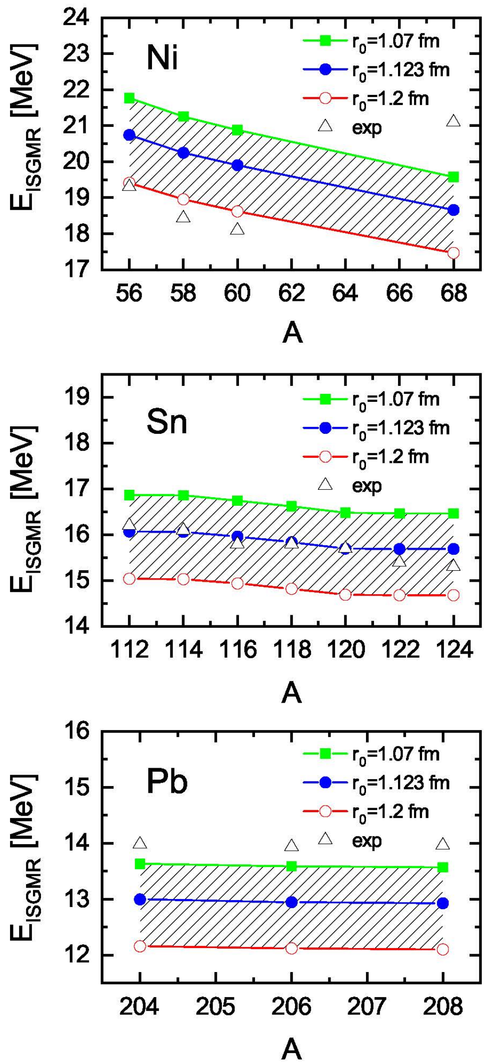


Figure 3. The centroid energies $E_{\rm ISGMR}$ as a function of the mass number $A$ for Ni, Sn, and Pb isotopes in the case of SLy4 force obtained with three different values of the parameter $r_0 = 1.07, 1.123, 1.2$ fm [Eq. (1)] compared with the experimental data.

calculated values of $E_{\rm ISGMR}$ and the corresponding ranges of change in respect to $r_0$ are illustrated in Figure 3 by hatched areas. Thus, we find a sensitivity of the results for centroid energies of ISGMR to the radial parameter $r_0$ and this fact has to be taken into account when considering resonances in light, medium, and heavy nuclei.

The calculated values of $E_{\text{ISGMR}}$ with SLy4 and SkM forces for Ca, Fe, Zn, Zr, Mo, and Cd isotopes are given in Tables 4 and 5, respectively. An excellent agreement with the available experimental data is achieved for Ca isotopic chain and also for Cd chain. For the latter case our results fit very well the theoretical predictions from QRPA calculations for the ISGMR peaks obtained with the SV-bas Skyrme force [70].

Table 4. The values of the centroid energies $E_{\text{ISGMR}}$ (in MeV) of Ca, Fe, Zn, Zr, and Mo isotopes obtained from HF+CDFM calculations in this work using SLy4 and SkM Skyrme forces and $r_0 = 1.2$ fm compared with the experimental data found in the literature.

| **Nucleus** | **SLy4** | **SkM** | **Exp.** |
|---|---|---|---|
| $^{40}$Ca | 20.03 | 19.99 | 19.18 ± 0.37 [24] |
| $^{42}$Ca | 19.83 | 19.98 | 19.7 ± 0.1 [68] |
| $^{44}$Ca | 19.71 | 19.95 | 19.49 ± 0.34 [17] |
| $^{46}$Ca | 19.69 | 19.91 | |
| $^{48}$Ca | 19.71 | 19.89 | 19.88 ± 0.16 [24] |
| $^{54}$Fe | 19.45 | 19.62 | 19.66 ± 0.37 [69] |
| $^{64}$Zn | 17.82 | 17.94 | 18.88 ± 0.79 [69] |
| $^{68}$Zn | 17.24 | 17.42 | 16.60 ± 0.17 [69] |
| $^{90}$Zr | 16.05 | 16.17 | 16.9 ± 0.1 [18] |
| $^{92}$Zr | 15.82 | 15.94 | 16.5 ± 0.1 [18] |
| $^{92}$Mo | 15.99 | 16.12 | 16.6 ± 0.1 [18] |
| $^{94}$Mo | 15.78 | 15.90 | 16.4 ± 0.2 [18] |
| $^{96}$Mo | 15.52 | 15.62 | 16.3 ± 0.2 [18] |

Table 5. The values of the centroid energies $E_{\text{ISGMR}}$ (in MeV) of Cd isotopes obtained from HF+CDFM calculations in this work using SLy4 and SkM Skyrme forces and $r_0 = 1.123$ fm. The experimental data are taken from Ref. [15].

| **Nucleus** | **SLy4** | **SkM** | **Exp.** |
|---|---|---|---|
| $^{106}$Cd | 16.15 | 16.27 | 16.27 ± 0.09 |
| $^{110}$Cd | 15.88 | 15.98 | 15.94 ± 0.07 |
| $^{112}$Cd | 15.73 | 15.89 | 15.80 ± 0.05 |
| $^{114}$Cd | 15.64 | 15.75 | 15.61 ± 0.08 |
| $^{116}$Cd | 15.49 | 15.67 | 15.44 ± 0.06 |

## 4 Conclusions and Future Work

We conducted a systematic investigation of the isoscalar giant monopole resonance in wide range of isotopes using the microscopic self-consistent Skyrme HF+BCS method and the coherent density fluctuation model. In the present calculations four different Skyrme parameter sets are used: SLy4, SGII, Sk3, and SkM. They are chosen since they were employed in our previous works and, more importantly, are characterized by different values of the nuclear matter incompressibility. The calculations are based on the Brueckner energy-density functional for nuclear matter.

The main results of the present work can be summarized as follows:

i) A very good agreement is achieved between the calculated centroid energies of the ISGMR and corresponding experimental values for Ni isotopes when $r_0 = 1.2$ fm. Especially this concerns the exotic double-magic $^{56}$Ni nucleus, for which the obtained (with SLy4 Skyrme force) value is 19.41 MeV, in consistency with the centroid position of the ISGMR found at $19.1 \pm 0.5$ MeV.

ii) The comparative analysis of the centroid energies in the case of Sn and Pb isotopes shows less agreement with $r_0 = 1.2$ fm, but still in acceptable limits.

iii) The agreement with the experimental values of $E_{\text{ISGMR}}$ can be improved also by varying the parameter $r_0$ in strong connection with the mass dependence of this parameter and its effect for the considered isotopes.

In general, the results obtained in the present work demonstrate the relevance of our theoretical approach to probe the excitation energy of the ISGMR in various nuclei. Our future goal is to extend this theoretical study by employing more realistic energy-density functionals for nuclear matter, from one side. For example, the role of microscopic three-body forces in the proposed approach to study the giant monopole resonances can be clearly revealed by applying the latest version of the Barcelona–Catania–Paris–Madrid nuclear EDF ( [71] and references therein) and particularly to treat successfully medium-heavy nuclei. In addition, a good choice could be the microscopic EOS derived by Sammarruca et al. [72] based on high-precision chiral nucleon-nucleon potentials at next-to-next-to-next-to-leading order (N$^3$LO) of chiral perturbation theory [73, 74]. Thus, by employing of microscopic input in the energy-density functionals for nuclear matter, a stronger connection with fundamental nuclear forces can be achieved. From another side, the important issue will be to expand the nuclear spectrum also to deformed nuclei, in which the breaking of spherical symmetry would play a role. In addition, to extract the isospin dependence of the incompressibility coefficient, a key ingredient in astrophysical studies, further theoretical investigations are needed to carry out calculations of the ISGMR for neutron-rich nuclei and to compare the results with the available experimental data.

## Bibliography


[1] A. Bohr, B. Mottelson *Nuclear Structure*; Benjamin: New York, NY, USA, 1975; Volume 2.

[2] M.N. Harakeh, A. van der Woude *Giant Resonances*; Oxford University Press: Oxford, UK, 2001.

[3] S. Brandenburg, R.D. Leo, A.G. Drentje, M.N. Harakeh, H. Janszen, A. van der Woude (1982) *Phys. Rev. Lett.* **49** 1687.

[4] F. Zwarts, A. Drentje, M. Harakeh, A. van der Woude (1983) *Phys. Lett. B* **125** 123.

[5] S. Brandenburg, R.D. Leo, A. Drentje, M. Harakeh, H. Sakai, A. van der Woude (1983) *Phys. Lett. B* **130** 9.

[6] S. Shlomo, D.H. Youngblood (1993) *Phys. Rev. C* **47** 529.

[7] D.H. Youngblood, H.L. Clark, Y.-W. Lui (1999) *Phys. Rev. Lett.* **82** 691.

[8] C. Monrozeau, E. Khan, Y. Blumenfeld, C.E. Demonchy, W. Mittig, P. Roussel-Chomaz, D. Beaumel, M. Caamano, D. Cortina-Gil, J.P. Ebran, *et al.* (2008) *Phys. Rev. Lett.* **100** 042501.

[9] S. Bagchi, J. Gibelin, M.N. Harakeh, N. Kalantar-Nayestanaki, N.L. Achouri, H. Akimune, B. Bastin, K. Boretzky, H. Bouzomita, M. Caamano, *et al.* (2015) *Phys. Lett. B* **751** 371.

[10] M. Vandebrouck, J. Gibelin, E. Khan, N.L. Achouri, H. Baba, D. Beaumel, Y. Blumenfeld, *et al.* (2014) *Phys. Rev. Lett.* **113** 032504.

[11] M. Vandebrouck, J. Gibelin, E. Khan, N.L. Achouri, H. Baba, D. Beaumel, Y. Blumenfeld, M. Caamano, L. Caceres, G. Colo, *et al.* (2015) *Phys. Rev. C* **92** 024316.

[12] J.P. Blaizot (1980) *Phys. Rep.* **64** 171.

[13] U. Garg, G. Colò (2018) *Prog. Part. Nucl. Phys.* **101** 55.

[14] T. Li, U. Garg, Y. Liu, R. Marks, B.K. Nayak, P.M. Rao, M. Fujiwara, H. Hashimoto, K. Nakanishi, S. Okumura, *et al.* (2010) *Phys. Rev. C* **81** 034309.

[15] D. Patel, U. Garg, M. Fujiwara, H. Akimune, G.P.A. Berg, M.N. Harakeh, M. Itoh, T. Kawabata, K. Kawase, B.K. Nayak, T. Ohta, H. Ouchi, J. Piekarewicz, M. Uchida, H.P. Yoshida, M. Yosoi (2012) *Phys. Lett. B* **718** 447.

[16] J.P. Blaizot, D. Gogny, B. Grammaticos (1976) *Nucl. Phys. A* **265** 315.

[17] J. Button, Y.-W. Lui, D.H. Youngblood, X. Chen, G. Bonasera, S. Shlomo (2017) *Phys. Rev. C* **96** 054330.

[18] K.B. Howard, U. Garg, Y.K. Gupta, M.N. Harakeh, (2019) *Eur. Phys. J. A* **55** 228.

[19] K.B. Howard, U. Garg, M. Itoh, H. Akimune, M. Fujiwara, T. Furuno, Y.K. Gupta, M.N. Harakeh, K. Inaba, Y. Ishibashi, *et al.* (2020) *Phys. Lett. B* **801** 135185.

[20] K.B. Howard, U. Garg, M. Itoh, H. Akimune, M. Fujiwara, T. Furuno, Y.K. Gupta, M.N. Harakeh, K. Inaba, Y. Ishibashi, *et al.* (2020) *Phys. Lett. B* **807** 135608.

[21] K.A. Brueckner, M.J. Giannoni, R.J. Lombard (1970) *Phys. Lett.* **31B** 97.

[22] S. Shlomo (2001) *Pramana-J. Phys.* **57** 557.

[23] L.-W. Chen, J.-Z. Gu (2012) *J. Phys. G* **39** 035104.

[24] M.R. Anders, S. Shlomo (2013) *J. Phys. Conf. Ser.* **420** 012051.

[25] J. Su, L. Zhu, C. Guo (2018) *Phys. Rev. C* **98** 024315.

[26] G. Colò, D. Gambacurta, W. Kleinig, J. Kvasil, V.O. Nesterenko, A. Pastore (2020) *Phys. Lett. B* **811** 135940.

[27] G. Bonasera, S. Shlomo, D.H. Youngblood, Y.-W. Lui, J. Button, X. Chen (2021) *Nucl. Phys. A* **1010** 122159.

[28] K.A. Brueckner, J.R. Buchler, S. Jorna, A.R.J. Lombard (1968) *Phys. Rev.* **171** 1188.

[29] K.A. Brueckner, J.R. Buchler, R.C. Clark, A.R.J. Lombard (1969) *Phys. Rev.* **181** 1543.

[30] A.N. Antonov, V.A. Nikolaev, I.Z. Petkov (1979) *Bulg. J. Phys.* **6** 151; (1980) *Z Phys. A* **297** 257; (1982) *ibid* **304** 239; (1985) *Nuovo Cimento A* **86** 23; A.N. Antonov *et al.* (1989)*ibid* **102** 1701; A.N. Antonov, D.N. Kadrev, P.E. Hodgson (1994) *Phys. Rev. C* **50** 164.

[31] A.N. Antonov, P.E. Hodgson, I.Z. Petkov *Nucleon Momentum and Density Distributions in Nuclei*; Clarendon Press: Oxford, UK, 1988.

[32] A.N. Antonov, P.E. Hodgson, I.Z. Petkov, *Nucleon Correlations in Nuclei*; Springer: Berlin/Heidelberg Germany; New York, NY, USA, 1993.

[33] J.J. Griffin, J.A. Wheeler (1957) *Phys. Rev.* **108** 311.

[34] A.N. Antonov, I.S. Bonev, C.V. Christov, I.Z. Petkov (1988) *Nuovo Cimento A* **100** 779.

[35] A.N. Antonov, V.A. Nikolaev, I.Z. Petkov (1991) *Bulg. J. Phys.* **18** 107.

[36] A.N. Antonov, M.K. Gaidarov, D.N. Kadrev, M.V. Ivanov, E. Moya de Guerra, J.M. Udias (2004) *Phys. Rev. C* **69** 044321.

[37] A.N. Antonov, M.K. Gaidarov, M.V. Ivanov, D.N. Kadrev, E. Moya de Guerra, P. Sarriguren, J.M. Udias (2005) *Phys. Rev. C* **71** 014317.

[38] A.N. Antonov, M.V. Ivanov, M.K. Gaidarov, E. Moya de Guerra, P. Sarriguren, J.M. Udias (2006) *Phys. Rev. C* **73** 047302.

[39] A.N. Antonov, M.V. Ivanov, M.K. Gaidarov, E. Moya de Guerra, J.A. Caballero, M.B. Barbaro, J.M. Udias, P. Sarriguren (2006) *Phys. Rev. C* **74** 054603.

[40] M.V. Ivanov, M.B. Barbaro, J.A. Caballero, A.N. Antonov, E. Moya de Guerra, M.K. Gaidarov (2008) *Phys. Rev. C* **77** 034612.

[41] A.N. Antonov, M.V. Ivanov, M.B. Barbaro, J.A. Caballero, E. Moya de Guerra, M.K. Gaidarov (2007) *Phys. Rev. C* **75** 064617.

[42] A.N. Antonov, M.V. Ivanov, M.B. Barbaro, J.A. Caballero, E. Moya de Guerra (2009) *Phys. Rev. C 79* 044602.

[43] J.A. Caballero, M.B. Barbaro, A.N. Antonov, M.V. Ivanov, T.W. Donnelly (2010) *Phys. Rev. C* **81** 055502.

[44] M.K. Gaidarov, A.N. Antonov, P. Sarriguren, E. Moya de Guerra (2012) *Phys. Rev. C* **85** 064319.

[45] M.K. Gaidarov, A.N. Antonov, P. Sarriguren, E. Moya de Guerra (2011) *Phys. Rev. C* **84** 034316.

[46] M.K. Gaidarov, P. Sarriguren, A.N. Antonov, E. Moya de Guerra (2014) *Phys. Rev. C* **89** 064301.

[47] Y.-W. Lui, D.H. Youngblood, H.L. Clark, Y. Tokimoto, B. John (2006) *Phys. Rev. C* **73** 014314.

[48] L.-G. Cao, H. Sagawa, G. Colò (2012) *Phys. Rev. C* **86** 054313.

[49] M. Fujiwara, T. Li, D. Patel, U. Garg, G.P.A. Berg, Y. Liu, R. Marks, J. Matta, B.K. Nayak, *et al.* (2011) *AIP Conf. Proc.* **1377** 164.

[50] D.H. Youngblood, Y.-W. Lui, H.L. Clark, B. John, Y. Tokimoto, X. Chen (2004) *Phys. Rev. C* **69** 034315.

[51] S. Stringari (1982) *Phys. Lett. B* **108** 232.

[52] M.K. Gaidarov, E. Moya de Guerra, A.N. Antonov, I.C. Danchev, P. Sarriguren, D.N. Kadrev (2021) *Phys. Rev. C* **104** 044312.

[53] A.E.L. Dieperink, Y. Dewulf, D. Van Neck, M. Waroquier, V. Rodin (2003) *Phys. Rev. C* **68** 064307.

[54] L.W. Chen (2011) *Phys. Rev. C* **83** 044308.

[55] I.C. Danchev, A.N. Antonov, D.N. Kadrev, M.K. Gaidarov, P. Sarriguren, E. Moya de Guerra (2020) *Phys. Rev. C* **101** 064315.

[56] D. Vautherin (1973) *Phys. Rev. C* **7** 296.

[57] E. Chabanat, P. Bonche, P. Haensel, J. Meyer, R. Schaeffer (1998) *Nucl. Phys. A* **635** 231.

[58] M. Beiner, H. Flocard, N.V. Giai, P. Quentin (1975) *Nucl. Phys. A* **238** 29.

[59] N.V. Giai, H. Sagawa (1981) *Phys. Lett. B* **106** 379.

[60] H. Krivine, J. Treiner, O. Bohigas (1980) *Nucl. Phys. A* **336** 155.

[61] A.N. Antonov, M.K. Gaidarov, P. Sarriguren, E. Moya de Guerra (2016) *Phys. Rev. C* **94** 014319.

[62] P. Sarriguren, M.K. Gaidarov, E. Moya de Guerra, A.N. Antonov (2007) *Phys. Rev. C* **76** 044322.

[63] P. Danielewicz, J. Lee (2009) *Nucl. Phys. A* **818** 36.

[64] B.A. Brown, C.R. Bronk, P.E. Hodgson (1984) *J. Phys. G* **10** 1683.

[65] R.-H. Li, Y.-M. Hu, M.-C. Li (2009) *Chin. Phys. C* **33** 123.

[66] J.D. Walecka *Theoretical Nuclear and Subnuclear Physics*; Oxford University Press: Oxford, NY, USA, 1995.

[67] J.M. Eisenberg, W. Greiner Nuclear Theory. *Excitation Mechanusms of the Nucleus*; In North-Holland Publishing Company: Amsterdam, The NEtherland; London, UK, 1970; Volume 2.

[68] K.B. Howard *et al.* (2020) *Phys. Lett. B* **801** 135185.

[69] J. Button *et al.* (2019) *Phys. Rev. C* **100** 064318.

[70] J. Kvasil, V.O. Nesterenko, A. Repko, W. Kleinig, P.-G. Reinhard (2016) *Phys. Rev. C* **94** 064302.

[71] B.K. Sharma, M. Centelles, X. Vi nas, M. Baldo, G.F. Burgio (2015) *Astron. Astrophys.* **584** A103.

[72] F. Sammarruca, L. Coraggio, J.W. Holt, N. Itaco, R. Machleidt, L.E. Marcucci (2015) *Phys. Rev. C* **91** 054311.

[73] R. Machleidt, D.R. Entem (2011) *Phys. Rep.* **503** 1.

[74] D.R. Entem, R. Machleidt (2003) *Phys. Rev. C* **68** 041001.